Carbohydrate Polymers 86 (2011) 1549–1557

Contents lists available at ScienceDirect

Carbohydrate Polymers

journal homepage: www.elsevier.com/locate/carbpol

HPMC reinforced with different cellulose nano-particles

Cristina Bilbao-Sainz [a,*], Julien Bras [b], Tina Williams [a], Tangi Sénechal [b], William Orts [a]

[a] Western Regional Research Center, ARS, U.S. Department of Agriculture, 800 Buchanan St, Albany, CA 94710, United States
[b] Ecole Internationale du Papier de la Communication Imprimée et des Biomatériaux, 461 rue de la Papeterie, Grenoble, France

ARTICLE INFO

Article history:
Received 9 April 2011
Received in revised form 10 June 2011
Accepted 21 June 2011
Available online 29 June 2011

Keywords:
HPMC
Cellulose
Nanoparticles
Nanocomposites
Barrier
Biodegradable packaging

ABSTRACT

Three different types of cellulose nanoparticles: (i) nano-fibrils cellulose (NFC), (ii) nano-fibrils cellulose oxidized using the tempo reaction (NFCt) and (iii) cellulose whiskers, were incorporated into HPMC edible films at different concentrations. The films were examined for mechanical and moisture barrier properties verifying how the addition of cellulose nano-particles affected the water affinities (water adsorption/desorption isotherms) and the diffusion coefficients. In general, addition of NFC or NFCt negatively affected the performance of the HPMC films. However the reinforcing effect of the cellulose particles was observed when whiskers were used as the filling material; an increase of 22% in tensile strength and 55% in Young's modulus were achieved while the elongation at break of the films was preserved. Addition of whiskers also improved the water barrier properties of the composite films. This effect was attributed to the lower water affinity of the composite films, as compared with the HPMC films, since the water diffusivity values were not affected by the addition of whiskers. Furthermore, the whiskers only decreased 3–6% the transparency of the HPMC films showing 86–89% visible light transmission values, allowing application as edible barrier and transparent film.

Published by Elsevier Ltd.

1. Introduction

Synthetic polymers, made almost entirely from chemicals derived from crude oil (McCarthy, 1993), are widely used as primary packaging in the food industry due to the large availability at relatively low cost and because their good mechanical performance and barrier properties. However, the large amount of synthetic polymers used for food packaging creates two major drawbacks: (i) they are obtained from geolocalized and non renewable fossil resources and (ii) at the end of their life, there is for most of them an accumulation of non-biodegradable wastes. To address these environmental issues, there is a well-known strategy from 1990s (Petersen et al., 1999) which consists in utilizing alternative raw materials such as bio-based packaging materials made from agro-industrial polymers obtained from renewable, abundant and low cost sources (Davis & Song, 2006; Mohanty, Misra, & Hinrichsen, 2000; Mohanty, Misra, & Drzal, 2002). Biopolymers, such as cellulose and its derivatives, may offer attractive alternatives as long as their properties can be tailored to specific end-use applications. Cellulose derivatives have been widely studied, and there are numerous industrial applications in fiber, film and gel-based materials. For example, long chain cellulose esters (Edgar et al., 2001; Heinze, Liebert, & Koschella, 2006) possess very well-known thermoplastic properties (Glasser, Samaranayake, Dumay, & Dave, 1995; Vaca-Garcia, Gozzelino, Glasser, & Borredon, 2003) and their characteristics as barrier materials have been recently analyzed (Bras, Vaca-Garcia, Borredon, & Glasser, 2007). Cellulose ethers are also strongly studied in barrier packaging. As they are often water-soluble, they are mostly used as coating (Coma, Sebti, Pardon, Deschamps, & Pichavant, 2001) or in the preparation of edible films with efficient oxygen and hydrocarbon barrier properties (Kamper & Fennema, 1984; Park, Weller, Vergano, & Testin, 1993).

Hydroxypropyl methylcellulose (HPMC) is one of the cellulose ethers which is the most commonly used. It is approved for food uses by the FDA (21 CFR 172.874) and the EU (EC, 1995) and it is used in the food industry as an emulsifier, protective colloid, stabilizer, suspending agent, thickener, or film former. The films obtained from HPMC are resistant to oils and fats, flexible, transparent, odorless, and tasteless but tend to have moderate strength (Krochta & Mulder-Johnston, 1997).

Indeed the use of agro-industrial biodegradable polymers has been limited because of problems related to performance such as brittleness and poor gas and moisture barrier. The application of nanotechnology by developing polymer nanocomposite films with the addition of fillers in the nanometric range may open new possibilities for improving these mechanical and barrier properties. The reinforcement is currently considered as a nanoparticle when at least one of its dimensions is lower than 100 nm. This particular feature provides nanocomposites unique and outstanding properties never found in conventional composites.

* Corresponding author. Tel.: +1 510 559 6190; fax: +1 510 559 5675.
E-mail address: cristina.bilbao@ars.usda.gov (C. Bilbao-Sainz).

0144-8617/$ – see front matter. Published by Elsevier Ltd.
doi:10.1016/j.carbpol.2011.06.060

New bio-based nanofillers coming from starch (Le Corre, Bras, & Dufresne, 2010), cellulose (Dufresne, 2006) or chitin (Qi, Xu, Jiang, Hu, & Xiangfei, 2004) have been more and more studied during last decade and present the advantage to be renewable, present anywhere, have low cost, have low density, be biodegradable and easily destroyed when incinerate at the end of life. Cellulose based nanoparticles are more and more developed with several recent reviews (Habibi, Lucia, & Rojas, 2010; Siro & Plackett, 2010) and expected industrialization in coming year. Most of the studies focus on their mechanical properties as reinforcing phase and their liquid crystal self-ordering properties (Siqueira, Bras, & Dufresne, 2010).

Moreover several kinds of nanocellulose can be reported. Up to now they are roughly categorized into three groups; (i) cellulose nanocrystals or cellulose nanowhiskers prepared by acid hydrolysis of native celluloses and successive mechanical agitation of the acid-hydrolyzed residues in water to obtain stiff rod-like nanocrystals (e.g. Dong, Revol, & Gray, 1998; Habibi et al., 2010; Marchessault, Morehead, & Walter, 1959), (ii) microfibrillated celluloses (MFCs) prepared by mechanical disintegration of cellulose/water slurries with or without energy-diminishable assistance by partial carboxymethylation or cellulase treatment (e.g. Henriksson, Henriksson, Berglund, & Lindström, 2007; Turbak, Snyder, & Sandberg, 1983), and (iii) cellulose nanofibrils prepared by 2,2,6,6-tetramethylpiperidine-1-oxy radical (TEMPO)-mediated oxidation of native celluloses followed by mechanical disintegration of the oxidized celluloses in water (e.g. Isogai, Saito, & Fukuzumi, 2011; Saito, Okita, Nge, Sugiyama, & Isogai, 2006).

The two last categories are shaped like nanofibrils with diameter lower than 100 nm but length close to micrometer. Most of scientific researches are focused on only one type of nanocellulose and there are very few papers comparing the impact of the different cellulose nanofillers. The first one (Siqueira, Bras, & Dufresne, 2009) was focused on mechanical properties of PCL-nanocomposites. Recently a study compared the Water sorption behavior and gas barrier properties of cellulose whiskers and microfibrils 100% films (Belbekhouche et al., 2010) but usually barrier properties are studied mainly on cellulose nanocomposite. For example the water vapor transmission rate of cellulose nanocrystals reinforced glycerin plasticized carboxymethyl cellulose (CMC) films was found to decrease slightly upon heat-treatment (Choi & Simonsen, 2006). Transport properties of poly(vinyl alcohol) (PVA) films cross-linked with poly(acrylic acid) (PAA) and reinforced with cellulose whiskers were studied, including water vapor transport rate and the transport of trichloroethylene (Paralikar, Simonsen, & Lombardi, 2008). Reduced moisture transport was reported upon filler addition and improved performance was obtained for surface carboxylated nanocrystals due to improved dispersion. Improved water vapor barrier properties of biopolymer films, such as mango puree based edible films (Azeredo et al., 2009) and glycerol plasticized chitosan films (Azeredo et al., 2010) were also reported. A recent study on whiskers-PLA nanocomposites (Oksman, Mathew, Bondeson, & Kvien, 2006) proves also the positive impact of cellulose nanofillers on barrier properties. However, none of them compared the different nanocellulose and up to our knowledge, nobody checked the impact of different cellulose nanofillers for edible films application.

Therefore, the objective of this work was to cast HPMC films reinforced with cellulose fibers: Nanofibrillated cellulose (NFC), TEMPO oxidized cellulose fibers (NFCt) or cellulose nanowhiskers at different concentrations and to determine tensile mechanical properties, water resistance and appearance of the resulting composite films to evaluate their potential as bio-based films.

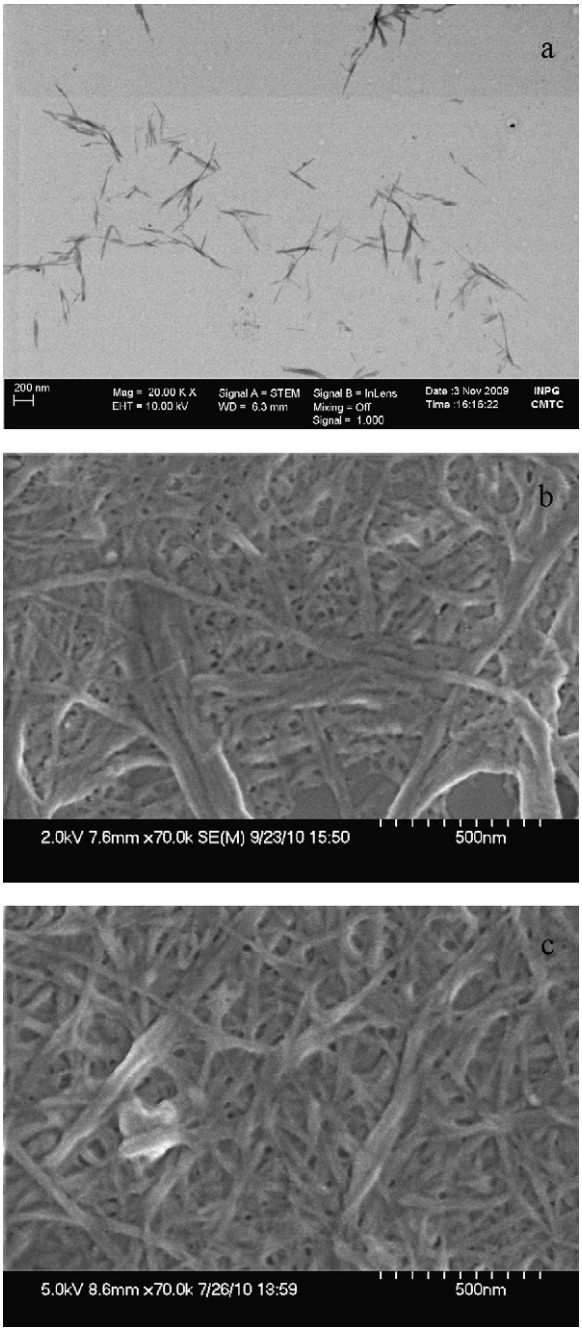

Fig. 1. Scanning electron micrographs (SEM-FEG) of cellulose whiskers (a), NFCt (b) and NFC (c).

2. Materials and methods

2.1. Preparation of nanofibrils cellulose (NFC)

Nanofibrillated cellulose suspension was produced from eucalyptus sulphite wood pulp (Fibria, Brazil). A suspension of bleached eucalyptus fibers (2.0% w/v) was pumped through a microfluidizer processor, Model M-110 EH-30. The slurry was passed through the valves that applied a high pressure. Size reduction of products occurs into Interaction Chamber (IXC) using cellules of different sizes (400, 200 and 100 μm). The fibers suspension was passed 3, 4 and 5 times through 400, 200 and 100 μm cellule containing in the Chamber fibrillation process respectively. Solid content of the suspension is around 2% (w/w).

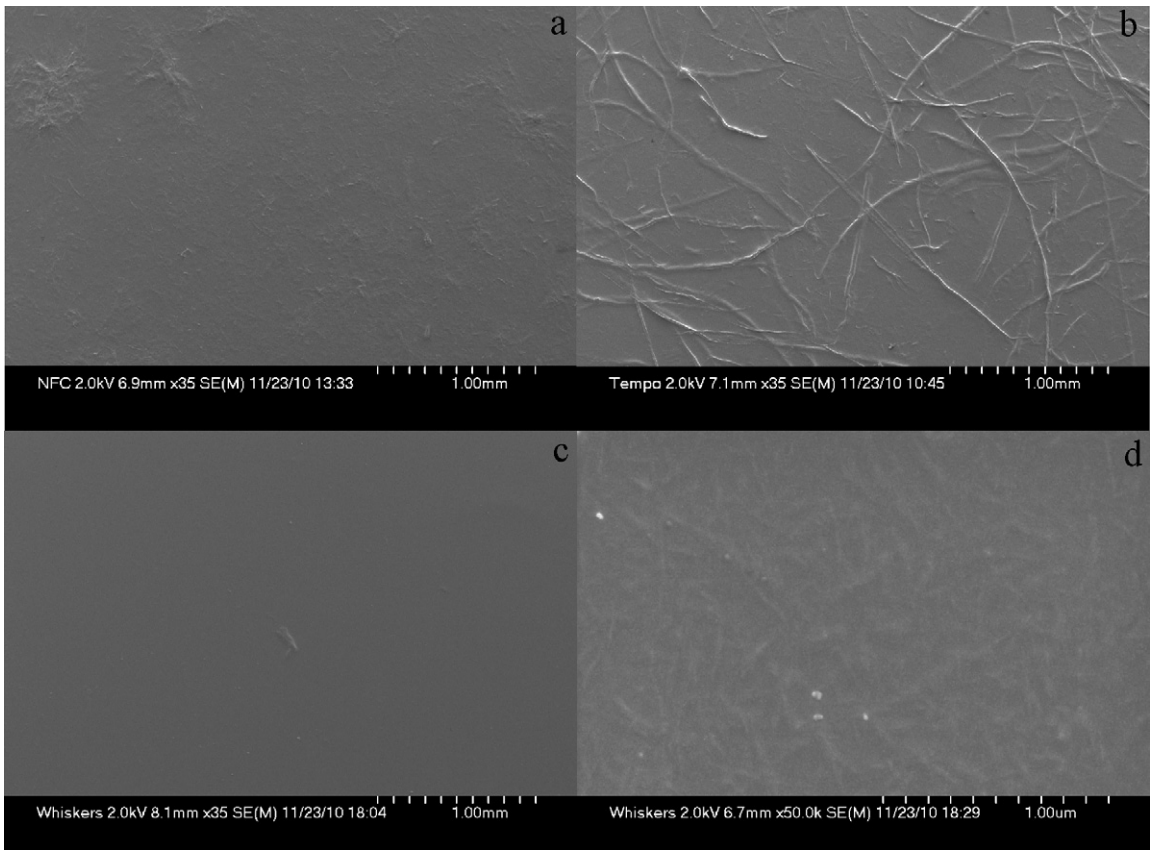

Fig. 2. SEM micrographs of HPMC films reinforced with cellulose fillers at the ratio 3 HPMC:0.4 filler. (a) HPMC:NFC; (b) HPMC:NFCt; (c) and (d) HPMC:cellulose whiskers.

2.2. Preparation of TEMPO-oxidized cellulose nanofibrils (NFCt)

The (2,2,6,6-tetramethylpiperidine-1-oxyl)-mediated (or TEMPO-mediated) oxidation has been used to convert the hydroxymethyl groups present on the cellulose fibers surface to their carboxylic form.

Softwood cellulose fibers 2.47 mm fiber length (Leaf River 90 Softwood Georgia-Pacific) were used as the cellulose source for TEMPO-mediated oxidation. TEMPO, sodium bromide, a 12% sodium hypochlorite solution, and other chemicals were of laboratory grade (Sigma–Aldrich). The 12% NaClO solution was adjusted to pH 10 by the addition of 0.1 M HCl before use.

The pulp cellulose (20 g) was suspended in water (2000 ml), then 0.32 g of TEMPO (0.016 g per gram of cellulose) and 2 g of sodium bromide (0.1 g per gram of cellulose) were dissolved in the cellulose suspension under agitation at 500 rpm. The TEMPO-mediated oxidation was started by adding 60 ml of 12% NaClO solution (3 ml per gram of cellulose) and was continued at room temperature by stirring at 500 rpm. The pH was maintained at 10 by adding 0.01 M NaOH using a pH stat until no NaOH consumption was observed, about 1 h. The pH was then adjusted to 7.5 with 0.5 M HCL. The TEMPO-oxidized cellulose was thoroughly washed with water by filtration and stored at 4 °C overnight before further treatment. 1% (w/v) slurry of TEMPO-oxidized cellulose in water was disintegrated at 1400 rpm for 1 h using a Polytron PT3100 homogenizer (Kinematica, Littau, Switzerland). The gel-like dispersion obtained was stored at 4 °C.

2.3. Preparation of cellulose nanowhiskers

Whiskers were prepared from microcrystalline cellulose using procedure described in Bondeson, Mathew, and Oksman (2006) study. MCC (100 g) and distilled water (350 g) were mixed before addition drop by drop of sulfuric acid at 96% (650 g). Temperature is controlled to avoid higher temperature than 60 °C. Suspension is heated at 44 °C during 130 min and mechanically stirred at 500 rpm.

The suspension was washed until neutrality by successive centrifugations at 10,000 rpm at 10 °C for 10 min each step and dialyzed against distillated water, in the sequence. Afterwards the whiskers suspension was homogenized by using an Ultra Turax T25 homogenizer for 5 min and filtered using glass filter no. 1. Some drops of chloroform were added to the whiskers suspension which was stored at 4 °C.Whiskers were sonicated to better disperse the nanocrystals before any use.

2.4. Preparation of composite films

Hydroxypropyl methyl cellulose (Methocel F50) was kindly provided by Dow Chemical Co. (Midland, MI). This HPMC is considered food grade. The control film forming solution was prepared by dissolving 3% HPMC in distilled water (w/w) using a hot/cold technique. The powder was first dispersed by mixing thoroughly with one-fifth to one-third of the total volume of water heated to above 90 °C until HPMC was thoroughly hydrated. The balance of water was added as cold water to lower the dispersion temperature. Once the dispersion reaches 70 °C, HPMC becomes completely water solubilized. The composite films forming solutions were prepared by adding cellulose particles suspension to HPMC solution to get final HPMC/filler ratios in the dried films of 3:0.08 and 3:0.4. The solutions were homogenized using a Polytron 3000 (Kinematica, Littau, Switzerland) at 10,000 rpm for 20 min. Vacuum was applied to degas the film forming solutions to prevent microbubble formation in the films. Glass casting plates (30 cm × 30 cm) with Mylar (polyester film, Dupont, Hopewell, VA) covers were used for film

casting. The mixes were cast to a wet thickness of 1.15 mm onto plates using casting bars, and the plates were allowed to dry at room temperature for 24 h. After drying, the films were removed from the Mylar.

2.5. Nanoparticles morphology analysis

The morphology of cellulose whiskers was investigated using a ZEISS-ULTRA55 scanning transmission electron microscope with field emission gun (SEM-FEG). The secondary electron detector INLENS SE 1 was located in the GEMINI column. It allows observation with a very low acceleration voltage of 1 kV and avoids degrading sensitive samples such as cellulose keeping a high resolution. The working distance was 6.3 mm.

The morphology of NFC and NFCt was measured using a Hitachi S-4700 field emission scanning electron microscope (Hitachi, Japan). The NFC and NFCt fiber solutions were prepared for observation, by dropping approximately 20 μl of each 0.01% solution onto a mica disk (Highest Quality Grade VI, Ted Pella, Inc., Redding, CA) previously attached to an aluminum specimen stub (Ted Pella, Inc.) with a double-adhesive coated carbon tab (Ultra Smooth Carbon Tabs, Electron Microscopy Sciences, Hatfield, PA). The samples were then coated with gold-palladium in a Denton Desk II sputter coating unit (Denton Vacuum, U.S.A., Moorestown, NJ). All samples were viewed and photographed at 2 kV and 5 kV.

2.6. Scanning electron microscopy (SEM) of composite films

Film surfaces were prepared for SEM by attaching the film directly to a stub with a carbon tab. Samples were coated with gold–palladium in a Denton Desk II sputter coating unit (Denton Vacuum, U.S.A., Moorestown, NJ). All samples were then viewed and photographed in a Hitachi S-4700 field emission scanning electron microscope (Hitachi, Japan) at 2 kV.

2.7. Water vapor permeability (WVP) determination

The gravimetric modified cup method based on ASTM E96-80 was used to determine WVP. Cabinets used to test final films contain fans operated by motors and variable speed controllers. The cabinets were kept at 25.3 ± 0.8 °C. Fan speeds achieved air velocities of 500 ft/min (152 m/min) to ensure uniform relative humidity (RH) throughout the cabinets. Cabinets were pre-equilibrated to 0%RH using calcium sulfate desiccant. Test cups were made from poly(methyl methacrylate) (Plexiglas). A film was sealed to the cup base with a ring containing a 19.6 cm^2 opening using four screws symmetrically located around the cup circumference. Deionized water was placed in the bottom of the test cup to expose the film to a high water activity inside the test cups. The films in the cup were oriented with the shiny side (the film side originally in contact with the Mylar cover) facing down (toward the inner, high-RH environment of the cup). Average stagnant air gap heights between the water and the film were determined. Eight test cups containing the same film were inserted into the pre-equilibrated 0%RH desiccator cabinets. Eight weights were taken for each cup at greater than 2 h intervals. For each experiment, the relative humidity at the film's underside and corrected WVP was calculated by the WVP correction method, accounting for the effect of the water vapor concentration gradient through the stagnant air layer in the cups (McHugh, Avena-Bustillos, & Krochta, 1993). Film thicknesses were measured to the nearest 0.001 mm at four positions around the film and in the center using a micrometer. Average values of the five thickness measurements per film were used in all WVP calculations.

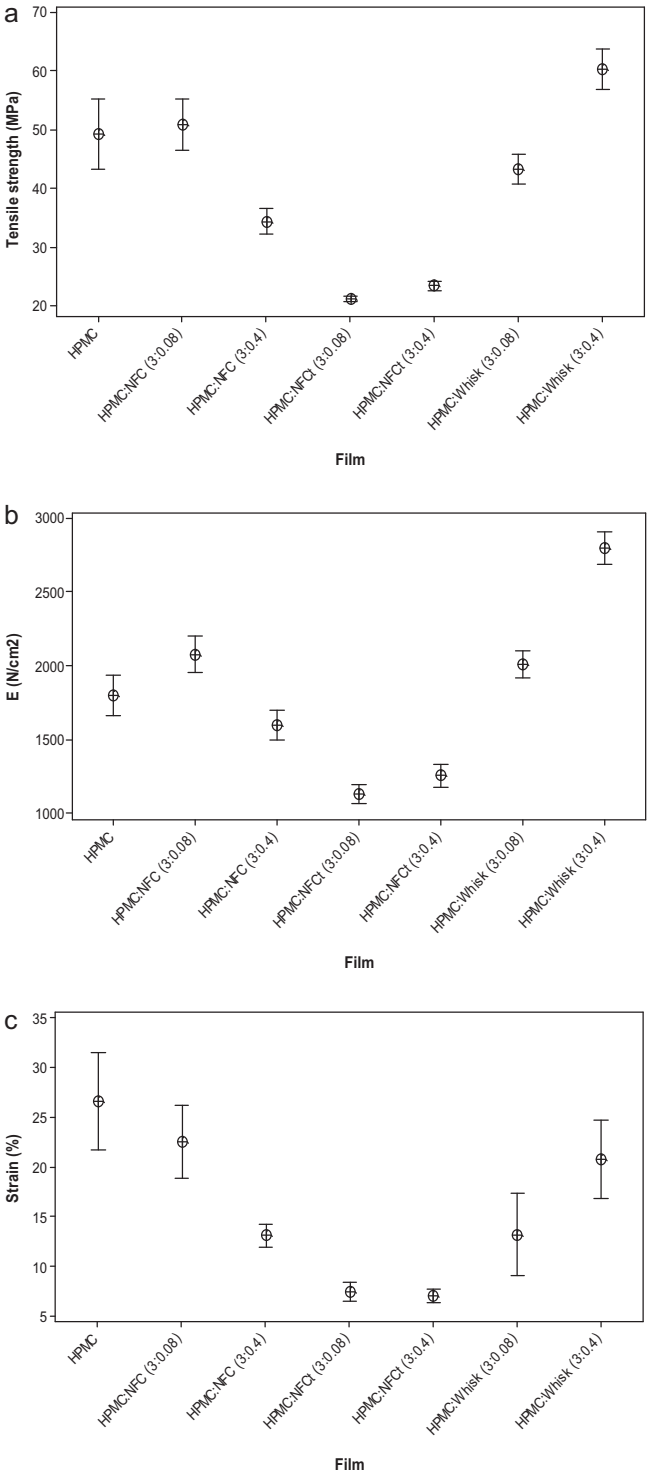

Fig. 3. Mechanical properties of hydroxypropyl methylcellulose (HPMC) films compounded with different cellulose nanoparticles (a) tensile strength, MPa; (b) Young's modulus, N/cm^2; (c) strain, %.

2.8. Mechanical property measurements

Films were cut to have a rectangular midsection of 15 mm wide by 100 mm long, flaring to 25 mm by 35 mm square sections on each end. At least 16 replicates of each film were tested. The cut films were then conditioned at 51% RH for 72 h using a saturated solution of $Ca(NO_3)_2{\cdot}4H_2O$ at 22 °C. This preconditioning before the tensile testing enables a true comparison of mechanical strength

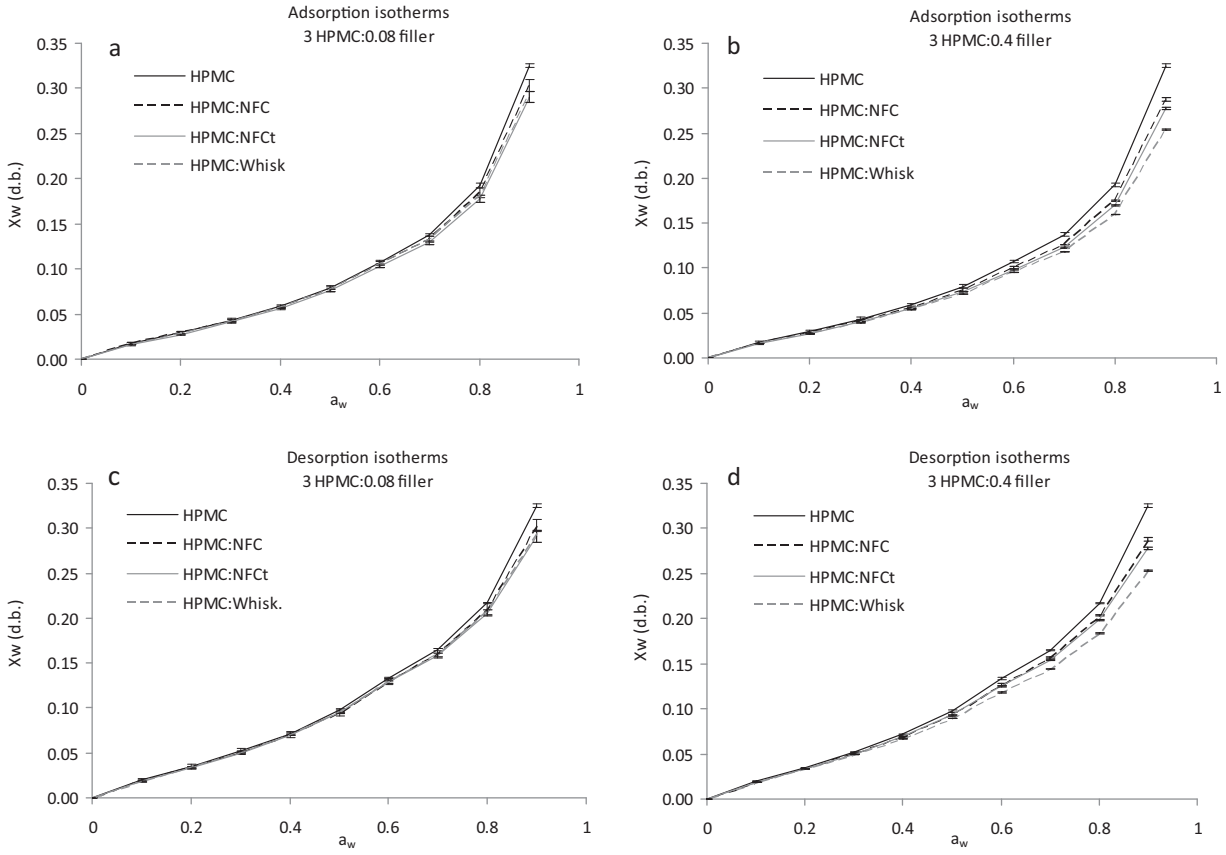

Fig. 4. Adsorption and desorption isotherms of HPMC films reinforced with different cellulose fillers.

of the films. An Instron Universal Testing Machine (model 1122, Instron Corp., Canton, MA) was used to determine the maximum TS (tensile strength) and maximum percentage elongation at break. The instrument was operated with self-alignment grips that consist of one fixed and one free end. The free end moves easily into alignment when load is applied. The mechanical properties were determined at 22 °C according to ASTM D882-97. The ends of the cut films were clamped with grips, and films were stretched using a speed of 50 mm/min.

Maximum tensile strength is the largest stress that a film is able to sustain against applied tensile stress before the film tears. Elongation at break is the maximum percentage change in the original film length before breaking. Young's modulus, calculated from the slope of the initial linear region of the stress–strain curves, reflects the film stiffness.

2.9. Film water affinity

Water transfer through the film occurs in three steps: first, water vapor condenses and dissolves on the high water concentration side of the film surface; second, water molecules move through the film, driven by a concentration or activity gradient; and third, water evaporates from the other side of the film (Krochta & Miller, 1997). Therefore, the factors describing the permeability process include the affinity between the water and the film material (adsorption/desorption) and the resistance of water movement in the polymeric network matrix, expressed as effective diffusivity (Larotonda, Matsui, Sobral, & Laurindo, 2005; Müller, Yamashita, & Laurindo, 2008; Müller, Laurindo, & Yamashita, 2009).

A dynamic vapor sorption analyzer DVS-1 (Surface Measurement Systems, Allentown, PA) was used to obtain the water adsorption/desorption isotherms of selected formulations. Each film was subjected to various conditions of relative humidity, and the response of the sample was measured gravimetrically over time until the sample reached equilibrium. The sample was exposed to a humidity range of 0–90%and then 90–0% again at 25 °C. Three replicates of each film were tested.

The Guggenheim–Anderson–de Boer (GAB) model (Eq. (1)) was used to represent the experimental equilibrium data. In this equation the parameter Xw is the equilibrium moisture (g of water/g of dry mass), M_0 is the monolayer water content, C is theGuggenheim constant, which represents the sorption heat of the first layer, and k is the sorption heat of the multilayer. The GAB model parameters were determined by polynomial regression using Microsoft Excel 2007.

$$X_w = \frac{C \times k \times M_0 \times a_w}{[(1 - ka_w) \times (1 - ka_w + Cka_w)]} \quad (1)$$

The method used to calculate the diffusion constants for the thin films uses diffusion equations first employed by Crank (1975). At short times, the initial kinetics of sorption into the bulk may be described by Eq. (2)

$$\frac{M_t}{M_\infty} = \frac{4}{L}\sqrt{\frac{D \times t}{\pi}} \quad (2)$$

where M_t = mass of water sorbed at time t, M_∞ = mass sorbed at thermodynamic equilibrium, L is the thickness of the film, and D is the diffusion coefficient. A diffusion coefficient is calculated for every relative humidity step from the slope by fitting a line M_t/M_∞ versus sqrt (time)/d, keeping the fitted R^2 over 99%.

2.10. Transparency of films

Film specimens were cut into rectangles (1 cm × 3 cm) and attached to a quartz spectrophotometer cell. The relative transparency was measured by transmittance (%) at selected wavelengths from 200 nm up to 800 nm using a UV–visible spectrophotometer (UV-1700, Shimadzu Corp., Kyoto, Japan). Three replicates of each film were tested.

3. Results and discussion

3.1. Characterization of the cellulose nanoparticles

SEM micrographs of whiskers reported in Fig. 1a shows the homogeneity and nanometric dimensions of the rigid rod-like whiskers. The length and diameter of nanocrystals were determined by using digital image analysis (ImageJ) with a minimum of 50 measurements. The geometric average length and diameter were around 301 ± 67 nm and 28 ± 9 nm, respectively. These dimensions are in agreement with the results classically found in literature (Bras, Viet, Bruzzese, & Dufresne, 2011).

Fig. 1b and c shows micrograph of NFC and NFCt respectively which proves the nanoscaled-fibrils shape with a diameter of 35 ± 9 nm and 67 ± 34 nm respectively. NFCt are then larger and more heterogeneous. Even some fibers at microscale have been observed with such material whereas NFC are more homogeneous with a well defined diameter.

3.2. Characterization of the composite films

Adding cellulose fiber reinforcement can improve functional properties of HPMC films, but fibers must be well dispersed to achieve any benefit. SEM micrographs of selected composite films at 3:0.4 HPMC:filler ratio are shown in Fig. 2. Fig. 2a shows that most of the nanofibrillated cellulose was evenly distributed within the HPMC polymeric matrix; however, some of the nanofibers appeared aggregated in clusters. When NFCt was used as the filling material (Fig. 2b), the film surface became rougher and the fillers were readily identifiable in the films. This confirms heterogeneity observed in the previous morphology analyses of nanofillers. On the contrary, the random orientation and the good dispersion of the cellulose whiskers in the HPMC matrices were evident (Fig. 2c and d). These results were a good indication of the excellent compatibility between the two components of the nanocomposite films that resulted in highly homogeneous materials and smooth surface films.

3.3. Mechanical properties

The reinforcement effect of the different cellulose nanoparticles on the mechanical properties of the HPMC nanocomposites films was evaluated up to their failure. Fig. 3a–c displays the tensile strength, the Young's modulus and the elongation at break as determined from the typical stress–strain curves of these materials.

The TS and the Young's modulus of the control HPMC film were 49.3 ± 6.5 MPa and 1804 ± 149 N/cm^2 respectively. The elongation at break of the same film was 26.5 ± 5.3%. One-way ANOVA indicated that the addition of whiskers to HPMC films resulted in significant improvements in film mechanical properties; the tensile strength of the HPMC films increased 22% with inclusion of whiskers at 3:0.4 HPMC:whiskers ratio and the Young's modulus increased 55% at the same HPMC:whiskers ratio. In addition, the elongation at break of the films was preserved with addition of cellulose whiskers. This enhancement was attributed to the high contact surface area of the smaller whiskers with the HPMC promoting the formation of hydrogen bonds between the HPMC and cellulose whiskers which might have lead to a higher efficiency of the stress transfer from the matrix to the fibers, however the addition of NFC or NFCt to the HPMC films did not result in any improvement in the mechanical properties or even had a detriment effect. This could be an indication of fewer interactions at the interface of both components due to the lower surface area, about 10 times lower for NFC in comparison with whiskers. Moreover the lower aspect ratio of NFC and NFCt and their flexibility favor an entanglement of NFC even at very low concentration. This entanglement is the main origin of the decrease of the elongation as already presented (Siqueira et al., 2009). However, for hydrogen bond formation between HPMC and NFCt, it would be better to prepare aqueous dispersions of NFCt with free carboxyl groups instead of sodium carboxylates. Sodium carboxylate groups cannot form hydrogen bonds with either hydroxyl or sodium carboxylate groups in NFCt-HPMC films (Fujisawa, Okita, Fukuzumi, Saito, & Isogai, 2011).

3.4. Effect of fillers on water vapor permeability of composite films

The effect of type of cellulose filler and concentration on water vapor permeability (WVP) of HPMC films was studied. Table 1 shows the WVP values where film thickness, water vapor transmission rate (WVTR) and relative humidity at the underside of the film are also included. Percentage RH at the film underside was not statistically different allowing a reliable comparison of WVP of the films, as different values of %RH of films have great influence in WVP of hydrocolloid films. Therefore WVP values were obtained at 25.3 ± 2.6 °C and a driving force gradient from 0% RH to 82.2 ± 0.8%RH in the film underside.

The WVP of HPMC films without fibers is 0.439 ± 0.03 g mm/kPa h m^2. In general, WVTR were quite similar for each sample. Nevertheless it was observed that the incorporation of NFC or NFCt in the HPMC films radically increased the film thickness and therefore WVP values. This might be due to the fact that all NFCs are in contact each other (entanglement) even at low concentration creating some preferential pathway for moisture. On the contrary a significant improvement in the WVP was obtained by adding whiskers to the HPMC films. This is due to the fact that we are under the percolation threshold of such nanowhiskers. In this case there is no preferential pathway and the impact is similar whatever the quantity. Indeed a very small quantity is sufficient to strongly change the tortuosity o the films. Sanchez-Garcia, Gimenez, and Lagaron (2008) reported that the presence of impermeable crystalline cellulose is thought to increase tortuosity in film matrixes, leading to slower diffusion processes and, hence, lower permeability.

3.5. Water adsorption/desorption isotherms of HPMC-based films

One factor that influences WVP is the interaction between the permeant (H_2O) and the HPMC matrix and cellulose nanofiller structures inside the HPMC matrix, resulting in differences in hygroscopicity (Müller et al., 2009). The adsorption/desorption isotherms at 25 °C are displayed in Fig. 4, which also includes the isotherm obtained for the unfilled HPMC films as a reference.

The adsorption and desorption isotherms acquired presented a slow initial increase in moisture content with water activity (a_w) increase up to 0.6 and a quick augmentation in film water adsorption with further rise of a_w implying a swelling phenomenon as water activity is increased and promoted solubilization. This behavior is characteristic of components rich in hydrophilic components and has been already reported in literature for HPMC based

Table 1
Comparison of WVP of HPMC reinforced with different concentrations of cellulose particles.

Film type	HPMC:filler ratio	Thickness (mm)	% RH film underside	WVTR (g/h m^2)	Permeability (g mm/kPa h m^2)
Control (3 wt% HPMC)		0.023 ± 0.002	81.5 ± 0.7	45.6 ± 1.8^a	0.44 ± 0.03^b
HPMC/NFC	3:0.08	0.024 ± 0.003	82.1 ± 2.1	44.1 ± 5.3^a	0.49 ± 0.06^b
	3:0.4	0.045 ± 0.005	81.9 ± 1.0	44.6 ± 2.4^a	0.70 ± 0.06^a
HPMC/NFCt	3:0.08	0.045 ± 0.001	81.7 ± 1.3	45.0 ± 3.1^a	0.75 ± 0.07^a
	3:0.4	0.050 ± 0.003	83.6 ± 0.9	40.5 ± 2.2^b	0.79 ± 0.04^a
HPMC/whiskers	3:0.08	0.028 ± 0.005	81.7 ± 0.7	45.0 ± 1.7^a	0.39 ± 0.03^c
	3:0.4	0.024 ± 0.001	83.3 ± 0.8	41.1 ± 2.0^b	0.38 ± 0.02^c

^{a,b}Different letters indicate significant differences at 95% confidence level.

Table 2
GAB model fitted parameters for sorption data from HPMC films with incorporation of cellulose nanofillers.

Film	GAB parameters			
	M_0 (g of water/g of solid)	C	k	R^2
HPMC	0.054 ± 0.001	3.42 ± 0.19	0.936 ± 0.003	0.969 ± 0.002
3 HPMC/0.08 NFC	0.053 ± 0.001	3.65 ± 0.11	0.932 ± 0.006	0.954 ± 0.008
3 HPMC/0.4 NFC	0.053 ± 0.001	3.53 ± 0.06	0.915 ± 0.008	0.946 ± 0.019
3 HPMC/0.08 NFCt	0.054 ± 0.001	3.38 ± 0.09	0.915 ± 0.001	0.962 ± 0.012
3 HPMC/0.4 MFCt	0.052 ± 0.001	3.65 ± 0.01	0.915 ± 0.002	0.958 ± 0.006
3 HPMC/0.08 whisk.	0.054 ± 0.003	3.27 ± 0.27	0.912 ± 0.007	0.951 ± 0.005
3 HPMC/0.08 whisk.	0.050 ± 0.001	3.82 ± 0.01	0.902 ± 0.001	0.939 ± 0.005

films (Sánchez-González, Vargas, González-Martínez, Chiralt, & Cháfer, 2009; Sebti, Ham-Pichavant, & Coma, 2002; Sebti, Chollet, Degraeve, Noel, & Peyrol, 2007; Villalobos, Hernández-Muñoz, & Chiralt, 2006).

The isotherms also show that addition of cellulose fillers contributed to a decrease in moisture uptake in the high a_w ranges ($a_w > 0.5$). At low filler concentration, similar equilibrium moistures were obtained regardless of the type of cellulose nanoparticles used. However at higher filler concentration, the water sorption isotherms of cellulose whiskers show clearly their lower water affinity as compared with NFC or NFCt. This could be attributed to the presence of more amorphous zones in these last two nanofibers (% crystallinity close to 70–80%) than in the whiskers (% crystallinity close to 95–100%). Amorphous zones as compared with crystalline regions will increase the swelling capacity of the polymer and therefore the amount of sorbed water.

The GAB model was used to fit the water adsorption data of the films in the 0–0.90 a_w range. Table 2 summarizes the constants for the GAB equation. The GAB model fit the HPMC film adsorption data very well as previously reported (Bilbao-Sainz, Avena-Bustillos, Wood, Williams, & McHugh, 2010; Villalobos et al., 2006). The effect of cellulose nanofiller inclusion on film hygroscopicity could also be observed from the monolayer water content data (M_0), this GAB parameter indicates the amount of water that is strongly adsorbed to specific sites. The monolayer water content for HPMC films without fillers was 0.054 g/g (db) and decreased significantly ($p < 0.05$) with the incorporation of whiskers at the higher concentration (3:0.4) down to 0.050 g/g (db). The lower water-binding capacity could be due to interactions between the whiskers and the hydrophilic sites of the HPMC chain, which substitute the HPMC–water interactions that predominate in films without inclusions. The monolayer moisture content tended to decrease with increasing nanoparticles concentration in the HPMC films, although this decrease was not statistically significant.

3.6. Effective water diffusion coefficient in films

Water permeation through edible films depends not only on the water adsorption and desorption but also on the water vapor diffusion inside the matrix. Fig. 5 shows the diffusivity values vs. a_w for the different nanocomposite films. A decrease in water vapor diffusivity with increasing moisture content was observed. According to Debeaufort, Voilley, and Meares (1994), these results may be explained by a clustering phenomenon. Once a monolayer of water molecules moistens the film, a further increase in moisture results in "free water" that does not interact with the polymer. The free water molecules aggregate to form di-, tri-, and tetramer clusters. The molecular volume of these clusters is larger than that of monomers and results in decreased diffusion.

Incorporation of NFC particles at high ratio (3:0.4) into HPMC films resulted in an increase in the water diffusion coefficient of HPMC/NFC films. In the same way incorporation of NFCt particles at low and high ratio also resulted in an increase in the diffusivity values. The larger diffusion coefficient could be due to the presence of amorphous zones that create a preferential pathway for the water vapor to diffuse. However, results did not show significant differences between diffusivities of films with different whiskers concentration as compared with the control HPMC film which seems to indicate the absence of pores in the composite film matrix.

3.7. Transparency/light transmission

Transparency of films is greatly relevant to the films functionality due to their great impact on the appearance of the products. Fig. 6 compares the % light transmission at selected wavelengths for all the samples in order to evaluate differences in their transparency.

Table 3
Effect of different cellulose fillers (HPMC:filler 3:0.4) on barrier, mechanical and optical properties of HPMC films.

Film type	WVP	Tensile strength	Young's modulus	Transparency
HPMC/NFC	+59%	−30%	−11%	−42%
HPMC/NFCt	+79%	−53%	−30%	−35%
HPMC/whiskers	−14%	+22%	+55%	−6%

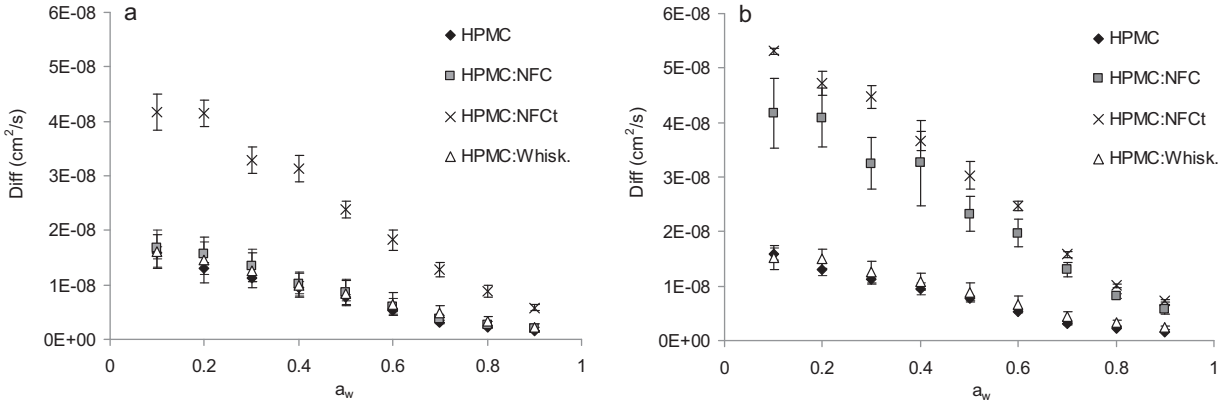

Fig. 5. Effect of type of cellulose filler on the water diffusion coefficient of HPMC-based films (a) 3 HPMC:0.08 filler ratio; and (b) 3 HPMC:0.4 filler ratio.

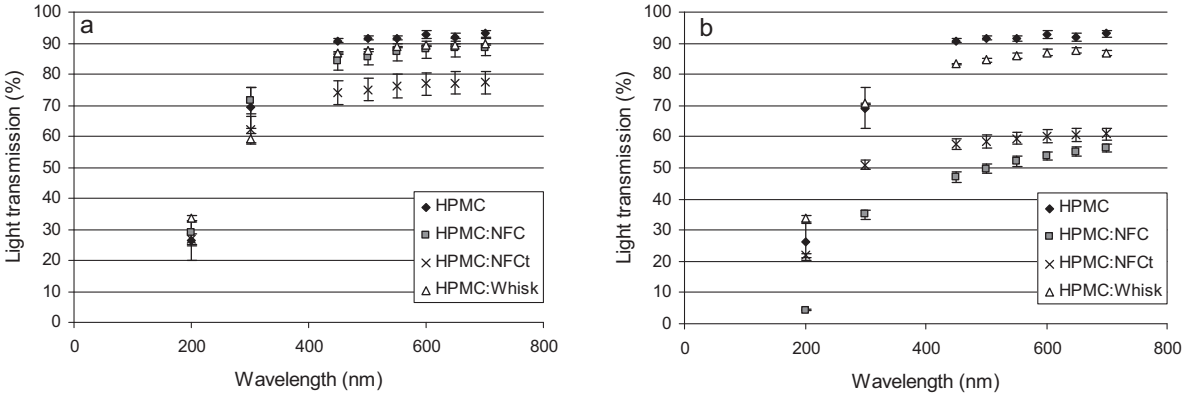

Fig. 6. Light transmission (%) of UV and visible for HPMC/cellulose fillers composite films. (a) 3 HPMC:0.08 filler ratio; and (b) 3 HPMC:0.4 filler ratio.

In the visible region (450–700 nm), the control HPMC film showed an excellent transparency characteristic (91.9 ± 0.8%). Addition of fillers had an effect on transmission percentage depending on the concentration and type of filler. Film transparency slightly decreased with the addition of NFC or NFCt at low concentration but drastically decreased at higher concentration since HPMC films containing NFC or NFCt showed minimum transmission values (52.4 ± 3.5% and 59.6 ± 1.3% respectively) probably due to the presence of solid particles (Fig. 2) leading to a strong deterioration of film transparency.

Fig. 6 also shows that the presence of cellulose whiskers slightly decreased the light transmittance of the HPMC films by 3% and 6% at low and high filler concentration respectively. The high values of light transmitted through the nanocomposites are due to the fine dispersion of the whiskers into the HPMC matrixes providing homogenous films with higher transparency values.

Comparing the transmittance of UV region with visible region (Fig. 6), it is noted that the rate of transmittance was lower at 200 nm and 300 nm, indicating that HPMC films and all composite films have a good preventive ability against radiation UV.

4. Conclusions

The composite produced by using whiskers as filling material were transparent, flexible and homogeneous; the nanocomposite films exhibited better water barrier and mechanical properties than HPMC films while decreasing only slightly the transparency of the films. However NFC and NFCt did not improve the performance of the HPMC films. Table 3 summarizes the barrier, mechanical and optical properties of the composite films as compared with HPMC films without any filler. These results indicate the great potential of HPMC/cellulose whiskers composite films for sustainable packaging applications.

References

Azeredo, H. M., Mattoso, L. H. C., Avena-Bustillos, R. J., Filho, G. C., Munford, M. L., & Wood, D. (2010). Nanocellulose reinforced chitosan composite films as affected by nanofiller loading and plasticizer content. *Journal of Food Science*, *75*(1), N1–N7.

Azeredo, H. M., Mattoso, L. H. C., Wood, D., Williams, T. G., Avena-Bustillos, R. J., & McHugh, T. H. (2009). Nanocomposite edible films from mango puree reinforced with cellulose nanofibers. *Journal of Food Science*, *74*(5), N31–N35.

Belbekhouche, S., Bras, J., Siqueira, G., Chappey, C., Lebrun, L., Khelifi, B., et al. (2010). Water sorption behaviour and gas barrier properties of cellulose whiskers and microfibrils films. *Carbohydrate Polymers*, *83*(4), 1740–1748.

Bilbao-Sainz, C., Avena-Bustillos, R. J., Wood, D. F., Williams, T., & McHugh, T. (2010). Composite edible films based on hydroxypropyl methylcellulose reinforced with microcrystalline cellulose nanoparticles. *Journal of Agriculture and Food Chemistry*, *58*(6), 3753–3760.

Bondeson, D., Mathew, A., & Oksman, K. (2006). Optimization of the isolation of nanocrystals from microcrystalline cellulose by acid hydrolysis. *Cellulose*, *13*(2), 171–180.

Bras, J., Viet, D., Bruzzese, C., & Dufresne, A. (2011). Correlation between stiffness of sheets prepared from cellulose whiskers and nanoparticles dimensions. *Carbohydrate Polymers*, *84*(1), 211–215.

Bras, J., Vaca-Garcia, C., Borredon, M. E., & Glasser, W. (2007). Oxygen and water vapor permeability of fully substituted long chain cellulose esters. *Cellulose*, *14*(4), 367–374.

Choi, Y. J., & Simonsen, J. (2006). Cellulose nanocrystal-filled carboxymethyl cellulose nanocomposites. *Journal of Nanoscience and Nanotechnology*, *6*(3), 633–639.

Coma, V., Sebti, I., Pardon, P., Deschamps, A., & Pichavant, F. H. (2001). Antimicrobial edible packaging based on cellulosic ethers, fatty acids, and nisin incorporation to inhibit Listeria innocua and Staphylococcus aureus. *Journal of Food Protection*, *64*(4), 470–475.

Le Corre, D., Bras, J., & Dufresne, A. (2010). Starch nanoparticles: A Review. *Biomacromolecules*, *11*(5), 1139–1153.
Crank, J. (1975). *The mathematics of diffusion* (2nd ed.). Oxford, U.K.: Clarendon Press.
Davis, G., & Song, J. H. (2006). Biodegradable packaging based on raw materials from crops and their impact on waste management. *Industrial Crops and Products*, *23*(2), 147–161.
Debeaufort, F., Voilley, A., & Meares, P. (1994). Water vapor permeability and diffusivity through methylcellulose edible films. *Journal of Membrane Science*, *91*(1–2), 125–133.
Dong, X. M., Revol, J., & Gray, D. G. (1998). Effect of microcrystallite preparation conditions on the formation of colloid crystals of cellulose. *Cellulose*, *5*(1), 19–32.
Dufresne, A. (2006). Comparing the mechanical properties of high performances polymer nanocomposites from biological sources. *Journal of Nanoscience and Nanotechnology*, *6*(2), 322–330.
Edgar, K. J., Buchanan, C. M., Debenham, J. S., Rundquist, P. A., Seiler, B. D., Shelton, M. C., et al. (2001). Advances in cellulose ester performance and application. *Progress in Polymer Science*, *26*(9), 1605–1688.
Fujisawa, S., Okita, Y., Fukuzumi, H., Saito, T., & Isogai, A. (2011). Preparation and characterization of TEMPO-oxidized cellulose nanofibril films with free carboxyl groups. *Carbohydrate Polymers*, *84*(1), 579–583.
Glasser, W. G., Samaranayake, G., Dumay, M., & Dave, V. (1995). Novel cellulose derivatives. III. Thermal analysis of mixed esters with butyric and hexanoic acid. *Journal of Polymer Science B: Polymer Physics*, *33*(14), 2045–2054.
Habibi, Y., Lucia, L. A., & Rojas, O. J. (2010). Cellulose nanocrystals: Chemistry, self-assembly, and applications. *Chemical Reviews*, *110*(6), 3479–3500.
Heinze, T., Liebert, T., & Koschella, A. (2006). *Esterification of polysaccharides*. Springer., 232pp.
Henriksson, M., Henriksson, G., Berglund, L. A., & Lindström, T. (2007). An environmentally friendly method for enzyme assisted preparation of microfibrillated cellulose nanofibers. *European Polymers Journal*, *43*(8), 3434–3441.
Isogai, A., Saito, T., & Fukuzumi, H. (2011). TEMPO-oxidized cellulose nanofibers. *Nanoscale*, *3*(1), 71–85.
Kamper, S. L., & Fennema, O. (1984). Water vapor permeability of an edible, fatty acid, bilayer film. *Journal of Food Science*, *49*(6), 1482–1485.
Krochta, J. M, & Miller, K. S. (1997). Oxygen and aroma barrier properties of edible films: A review. *Trends in Food Science and Technology*, *8*(7), 228–237.
Krochta, J. M., & Mulder-Johnston, C. (1997). Edible and biodegradable polymer films: Challenges and opportunities. *Food Technology*, *51*(2), 61–75.
Larotonda, F. D. S., Matsui, K. N., Sobral, P. J. A., & Laurindo, J. B. (2005). Hygroscopicity and water vapor permeability of Kraft paper impregnated with starch acetate. *Journal of Food Engineering*, *71*(4), 394–402.
Marchessault, R. H., Morehead, F. F., & Walter, N. M. (1959). Liquid crystal systems from fibrillar polysacchrides. *Nature*, *184*(9), 632–633.
McCarthy, S. P. (1993). *Biodegradable polymers for packaging in biotechnological polymers conference proceedings* Lancaster, PA, (pp. 214–222).
McHugh, T. H., Avena-Bustillos, R. J., & Krochta, J. M. (1993). Hydrophilic edible films: Modified procedure for water vapor permeability and explanation of thickness effects. *Journal of Food Science*, *58*(4), 899–903.
Mohanty, A. K., Misra, M., & Drzal, L. T. (2002). Sustainable bio-composites from renewable resources opportunities and challenges in the green material world. *Journal of Polymers and the Environment*, *10*(1–2), 19–26.
Mohanty, A. K., Misra, M., & Hinrichsen, G. (2000). Biofibres, biodegradable polymers and biocomposites: An overview. *Macromolecular Materials and Engineering*, *276–277*(1), 1–24.
Müller, C. M. O., Laurindo, J. B., & Yamashita, F. (2009). Effect of cellulose fibers addition on the mechanical properties and water vapor barrier of starch-based films. *Food Hydrocolloids*, *23*(5), 1328–1333.
Müller, C. M. O., Yamashita, F., & Laurindo, J. B. (2008). Evaluations of the effect of glycerol and sorbitol concentration and water activity on the water barrier properties of cassava starch films through a solubility approach. *Carbohydrate Polymers*, *72*(1), 82–87.
Oksman, K., Mathew, A. P., Bondeson, D., & Kvien, I. (2006). Manufacturing process of cellulose whiskers/polylactic acid nanocomposites. *Composites Science and Technology*, *66*(15), 2776–2784.
Paralikar, S. A., Simonsen, J., & Lombardi, J. (2008). Poly(vinyl alcohol)/cellulose nanocrystal barrier membranes. *Journal of Membrane Science*, *320*(1–2), 248–258.
Park, H. J., Weller, C. L., Vergano, P. J., & Testin, R. F. (1993). Permeability and mechanical properties of cellulose-based edible films. *Journal of Food Science*, *58*(6), 1361–1364.
Petersen, K., Nielsen, P. V., Bertelsen, G., Lawther, M., Olsen, M. B., Nilsson, N. H., et al. (1999). Potential of biobased materials for food packaging. *Trends in Food Science and Technology*, *10*(2), 52–68.
Qi, L., Xu, Z., Jiang, X., Hu, C., & Xiangfei, Z. (2004). Preparation and antibacterial activity of chitosan nanoparticles. *Carbohydrate Research*, *339*(16), 2693–2700.
Saito, T., Okita, Y., Nge, T. T., Sugiyama, J., & Isogai, A. (2006). TEMPO-mediated oxidation of native cellulose: Microscopic analysis of fibrous fractions in the oxidized products. *Carbohydrate Polymers*, *65*(4), 435–440.
Sanchez-Garcia, M. D., Gimenez, E., & Lagaron, J. M. (2008). Morphology and barrier properties of solvent cast composites of thermoplastic biopolymers and purified cellulose fibers. *Carbohydrate Polymers*, *71*, 235–244.
Sánchez-González, L., Vargas, M., González-Martínez, C., Chiralt, A., & Cháfer, M. (2009). Characterization of edible films based on hydroxypropylmethylcellulose and tea tree essential oil. *Food Hydrocolloids*, *23*(8), 2102–2109.
Sebti, I., Chollet, E., Degraeve, P., Noel, C., & Peyrol, E. (2007). Water sensitivity, antimicrobial, and physicochemical analyses of edible films based on HPMC and/or chitosan. *Journal of Agriculture and Food Chemistry*, *55*(3), 693–699.
Sebti, I., Ham-Pichavant, F., & Coma, V. (2002). Edible bioactive fatty acid-cellulosic derivative composites used in food-packaging applications. *Journal of Agriculture and Food Chemistry*, *50*(15), 4290–4294.
Siqueira, G., Bras, J., & Dufresne, A. (2010). Cellulosic bionanocomposites: A review of preparation, properties and applications. *Polymers*, *2*(4), 728–765.
Siqueira, G., Bras, J., & Dufresne, A. (2009). Cellulose whiskers vs. microfibrils: Influence of the nature of the nanoparticle and its surface functionalization on the thermal and mechanical properties of nanocomposites. *Biomacromolecules*, *10*(2), 425–432.
Siro, I., & Plackett, P. (2010). Microfibrillated cellulose and new nanocomposite materials: A review. *Cellulose*, *17*(3), 459–494.
Turbak, A. F., Snyder, F. W., & Sandberg, K. R. (1983). *Microfibrillated cellulose*, US patent 4374702.
Vaca-Garcia, C., Gozzelino, G., Glasser, G., & Borredon, M. E. (2003). Dynamic mechanical thermal analysis transitions of partially and fully substituted cellulose fatty esters. *Journal of Polymer Science B: Polymer Physics*, *41*(3), 281–288.
Villalobos, R., Hernández-Muñoz, P., & Chiralt, A. (2006). Effect of surfactants on water sorption and barrier properties of hydroxypropylmethylcellulose films. *Food Hydrocolloids*, *20*(4), 502–509.